# SYNTHESIS AND CHARACTERIZATION OF UNSUPPORTED CATALYST FOR GAS OIL DESULFURIZATION

**Mohammad F. Abid[*], Mohammed A. Hamza[*1], Shakir M. Ahmed[2], Salah M. Ali[3], Sattar J. Hussein[4]**

(*)Department of Chemical Engineering, University of Technology, Baghdad, Iraq.

E-mail: 80005@uotechnology.edu.iq

(*1)Department of Chemical Engineering, University of Technology, Baghdad, Iraq.

E-mail: m.alshmary35@@gmail.com

(2)SCOP, Ministry of Oil, Baghdad, Iraq.

E-mail: shakir58scop@gmail.com

(3)Petroleum Research and Development Center, Ministry of Oil, Baghdad, Iraq.

E-mail: salah56ali@yahoo.com

(4)Petroleum Research and Development Center, Ministry of Oil, Baghdad, Iraq.

E-mail: sattarjaleel@yahoo.com

**Abstract:** Unsupported $MoS_2$ catalysts were synthesized for the hydrodesulfurization (HDS) of real feed gas oil using different temperatures and pressures. Hydrothermal method was utilized to prepare by using molybdenum trioxide and sodium sulfide. The characterization of the catalyst was identified by XRD, SEM, and BET techniques. It was found that BET surface and pore volume were positively affected by pressure and temperature that could improve the activity of $MoS_2$. Kinetic analysis showed that HDS reaction over $MoS_2$ follow pseudo-first order kinetics. Experimental results revealed that the HDS activity of the unsupported $MoS_2$ catalyst was better than supported $CoMo/Al_2O_3$ catalyst under the same operating conditions.

**Keywords:** unsupported catalyst; middle distillates; hydrodesulfurization; hydrothermal method; catalyst activity.

## 1. INTRODUCTION

Recently, the request of fuel has been rising highly due to increase of automobile engines. However, the environmental regulation laws require motor fuels of low sulfur content which needs efficient and feasible hydrodesulfurization process. Consequently, petroleum refineries pay more attention to lower sulfur level in their products. The synthesis of new catalysts and utilizing modern refineries is the most acceptable solution to attain lowest sulfur levels.Most of the classical catalysts utilize in the hydrodesulfurization reactions are $CoMoS_2$, $MoS_2$ or $NiMoS_2$ supported on alumina **(Girgis and Gates, 1991; Speight and Ozum, 2001)**. In 2001, a new type of catalyst is synthesized in the market which is the unsupported catalyst **(Eijsbouts et al., 2007)**. Such catalysts have higher concentration of active sites per unit surface area of the catalyst, thus offer more activity than supported catalysts. Consequently, the synthesis of new unsupported sulfided catalyst appears to be a good required research trend. Improvement of catalyst activity depends on knowing the connection between the active sites and the framework of $MoS_2$ and $MoS_2$ catalysts. Although some published data have notified the framework-activity connections for $MoS_2$ and $CoMoS_2$ catalysts, they essentially concentrated upon the HDS process **(Hensen et al., 2001; Schweiger et al., 2002)**. These reports have depicted that the catalytic performance is quite related to the rims of the levels of the $MoS_2$ layers, and particularly with the sulfur-free places that are created over the rim sites. Many methods have emerged to synthesize $MoS_2$ or $CoMoS_2$ with controlled surface-characteristics, such as solvothermal **(Duphil et al., 2002)**, sonochemical **(Dhas and Suslick, 2005)** or biotemplate **(Chang et al., 2006)** syntheses. **Théodet (2010)** indicated that the activity of supported catalyst would be decreased due to the interference effect of the support with the active phase. Additionally, the concentration of active sites per unit volume is decreased thus high amounts of catalysts are required to attain the wanted fuel properties. The author depicted that bulk catalysts are the "wave of the future" in many industrial applications. **Avarez et al. (2008)** prepared unsupported $NiMoS_2$ catalyst from ammonium and C16H37NO, $(NH_4)_2MoS_4$ fattened with Ni(NO3)2.Authors depicted that the alkyl group in the $C_{16}H_{37}NO$ precursor had a direct effect on surface-characteristics of catalyst. The extent of the alkyl concatenation from C1 to C4 showed a very high HDS activity. **Gaojun et al. (2010)** prepared bulk $Ni-Mo-S_2$ catalyst. Their outcomes depicted that the bulk NiMo catalyst has excellent hydrogenation performance to produce fuel with sulfur content ≤ 10 ppm. **He and Que (2016)** provided a thorough review of the bulk $MoS_2$, briefing updated studies on framework, characteristics, preparation methods. The main aim of this study was to prepare and identify an unsupported catalyst (e.g., $MoS_2$). The other objective was to evaluate the performance of $MoS_2$ catalyst for HDS process of gas oil.

## 2. EXPERIMENTAL WORK

### 2.1 MATERIALS

Molybdenum oxide, ($MoO_3$, 99.5 wt%) was purchased from Merck. Sodium sulfide ($Na_2S$) (purity 62 wt%) was purchased from HRD, Germany. HCl (36 wt%) and ethanol (99.5 wt%) were obtained from CDH, India. Gas oil was obtained from Al-Daura Refinery, Baghdad. Properties of (gas oil) utilized in the present study was shown in Table (1).

Table (1): Properties of gas oil (Al-Daura Refinery, Baghdad)

| Property | Value |
|---|---|
| API @15.6 $^0$C | 40.1 |
| SP.GR @ 15.6 $^0$C | 0.8246 |
| Sulfur content (ppm) | 4940 |
| Cetane number | 51 |
| Distilled (vol.%) in crude oil | 17.1 |

| Property | Value |
|---|---|
| I.B.P ($^o$C) | 195 |
| E.B.P ($^o$C) | 322 |

## 2.2 CATALYST PREPARATION

$MoS_2$ was synthesized by a hydrothermal method using 1L stainless steel autoclave reactor (Model: Kurla (W), Mumbai-400070, India). A schematic of the synthesis setup was seen in Figure (1). Figure (2) represents a block diagram of the synthesis procedure. 0.0378 moles $MoO_3$ and 0.1415 moles $Na_2S.9H_2O$ were dissolved in 0.3L distilled water by stirring for 10 minutes to ensure homogeneous solution formation and then slowly 0.0425 ml of 4 M HCl solution was added. A black solution was formed by adding HCl. The solution was putted into an autoclave reactor and reacted at 280-320 $^{\circ}$C and 25-35 bars at 500 rpm for 120 minutes. Thereafter, the reactor was instantly cooled down by using a chiller. Black solid particles resulted from the synthesis was filtered and washed several times with deionized water and ethanol, and dried under nitrogen of atmosphere pressure at 160 °C for 240 minutes **(Zhang et al., 2015)**.
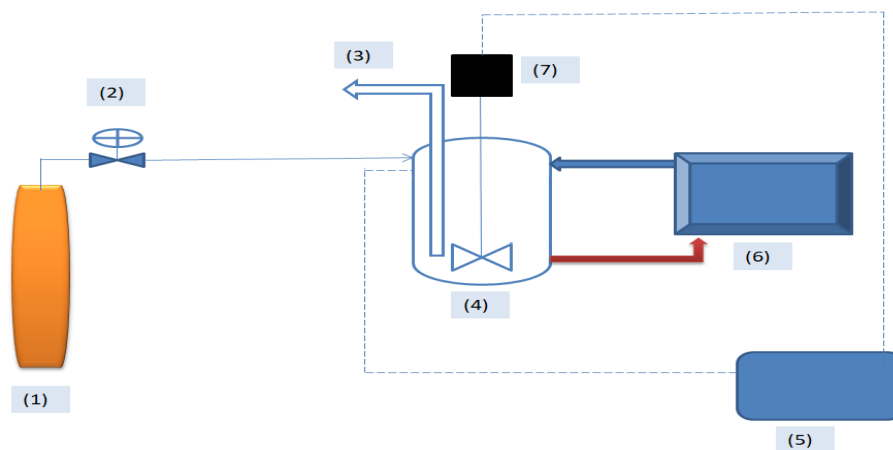


1- $N_2$ gas; 2- Gas pressure regulator; 3-sampling valve; 4-Batch reactor with heat and mixing component; 5- Temperature and speed control system; 6-chiller; 7- motor stirrer.

Figure (1): Schematic of the synthesis setup.
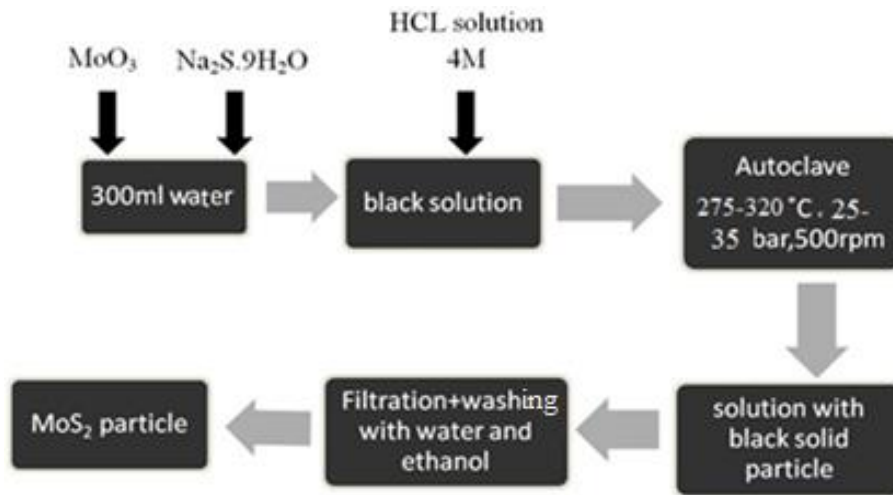
Figure (2): Block diagram for the production of MoS$_2$ catalyst.

## 2.3 IDENTIFICATION OF CATALYST

XRD analysis of MoS$_2$ was conducted using a diffraction unit [Shimadzu-6000, Japan]. X-Ray diffractometer (XRD) with a 2Ө range from 10o to 80o with scan rate 2 (deg/min) and Cu-kα (λ = 1.541 Å) as radiation source was applied. The analysis was carried out at the central service Laboratory in the University of Baghdad. Morphology analysis of MoS$_2$ was performed using SEM instrument [VEGA 3 LM, Germany] at the University of Technology. The specific surface area and pore volume of MoS$_2$ catalyst were determined utilizing Brunauer Emmett and Teller (BET) method using analyzer (Q Surf 1600, USA).The instrument is available in the Petroleum Research and Development Centre in Baghdad.

## 2.4 EXPERIMENTAL SETUP FOR KINETIC STUDY AND CATALYST ACTIVITY

The reactor was charged with MoS$_2$ (0.5 gm), and 100 ml of gas oil (GO). Seal test was conducted on reactor by purging several times with hydrogen and then raised pressure to 35 atm with stirring 600 rpm which ensure of getting rid of mass transfer resistance. Operating Temperature was varied at 300- 360oC. H$_2$ was fed continuously during the test in order to shun the decreasing of H$_2$ pressure due to the reaction. As the reaction continued samples were drawn periodically. The influence of sampling on mixture volume was neglected because of the small sample amounts (≤ 1.0 ml per sample). Sulfur analyzer (XOS, Sindie OTG, USA) was used to measure sulfur concentration in drawn samples. The sulfur removal is calculated from equation (1).

$$x \% = \frac{C_f - C(t)}{C_f} * 100 \qquad (1)$$

Where Cf and C(t) are initial and instantaneous sulfur concentrations respectively.

# 3. RESULTS AND DISCUSSION

## 3.1 EFFECT OF OPERATING PARAMETERS ON CATALYST CHARACTERISTICS

### 3.1.1 Influence of Temperature

Figures (3a) and (3b) demonstrate XRD images for the effect of temperature (300 and 320 oC), at constant pressure (35 bars), on crystalline structure and phase purity of $MoS_2$ nanostructures. As could be seen, all peaks presented in the two images have nearly the same locations on the 2 $\theta$-axis. However, at 300 oC, a small peak appears at 56.6∘, seen as left shift of 110 lattice facets. The spectra indicate a more amorphous-like $MoS_2$ (Fig. 3a-$MoS_2$) structure at low temperature. When the synthesis temp increases to 320∘C, a crystalline structure (denoted as Fig. 3b-$MoS_2$ hereafter) starts to develop, manifested by the characteristic peaks for 002, 100, 103, and 110 facets (Fig. 3a-b).The broad peaks, on the other hand, also reveal poor crystallite structure. The peak intensities were enhanced with increased synthesis temperature. As the temperature increased from 300 to 320 oC, the corresponding 2θ reflections became sharper and could be clearly observed. Moreover, sizes of peaks in Fig. 3a are smaller than in Fig. 3b, indicating that Mo and S powders could not completely react at the lower temperature. This confirmed the predominant effect of temperature on the yield of $MoS_2$. As can be observed in Figure 3b, the XRD peaks can be recorded to those of the perspicuous hexagonal phase of $MoS_2$ with lattice coefficients a = 3.161 Å, c = 12.84 Å, which are agree well with the amounts of standard card (JCPDS No. 37-1492). No featured peaks were revealed from other impurities, pointing out that the sample has high purity. The application of XRD showed that the crystal structure of the particles was hexagonal. Additionally, the comparison of the obtained peaks in Figures 3a and 3b indicated that the $MoS_2$ nanoparticles average particle size was calculated, according to Scherer's equation (Eq. 2), approximately as 32 and 21nm at temperatures of 300 and 320 oC respectively.

$$D = \frac{0.9\,\gamma}{\beta\,cos\theta} \tag{2}$$

Where D is the mean crystalline size (nm), $\gamma$ is the wavelength of Cu Ka (0.154 nm), $\beta$ is the full width at half maximum intensity (FWHM) in radian and $\theta$ is the Bragg angle.However, **Choi et al. (2018)** reported that the rising of synthesis temperature increases the reaction rate of $MoO_3$ to $MoS_2$ it decreases the number of active sites available for the reaction. These findings of Choi et al. confirmed that there is an optimum temperature for the synthesis of the catalyst.
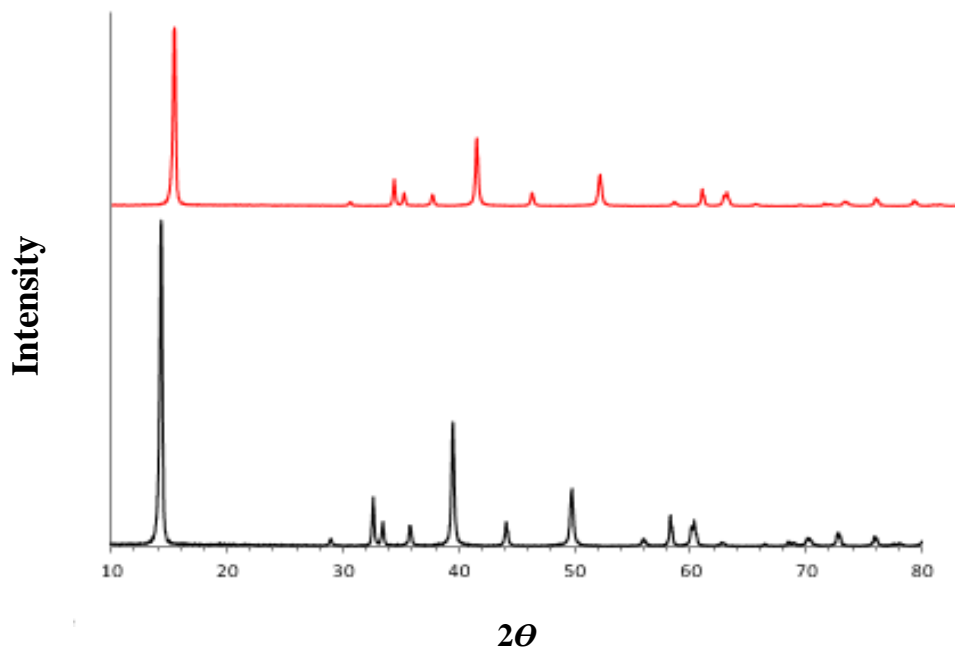
Figure (3): XRD images (a) at 300 ∘C & 35 bar and (b) at 320 ∘C & 35 bar.

### 3.1.2 Influence of Pressure

Figure (4a) and (4b) demonstrates XRD images for the effect of pressure (25 and 35 bar) at constant temperature (280 ᵒC). The main perceptible XRD peaks can be easily recorded to the hexagonal phase of MoS2 compatible with the standard powder XRD folder of $MoS_2$ (JCPDS 37-1492), and there is peak from impurity due to incomplete $MoO_3$ conversion. Moreover, the strength of the XRD peaks of $MoS_2$ varied significantly under different imposed pressures. With further increasing of the reaction pressure to 35 bars, XRD pattern (Figure. 4b) shows that the intensities of XRD peaks of $MoS_2$ increase. As seen in Figure 4, the higher and acute peaks depict that the sample was quite crystallized. The higher the imposed pressure is, the better the crystallized products will be. Sulfur concentration on Mo films is related to the dynamic pressure within the reactor. By increasing the pressure, the concentration of sulfur on Mo surface increases, therefore, a higher nucleation density of $MoS_2$ was expected on the Mo film. These nucleation sites cannot proceed further when low pressure applied because of low sulfur concentration at Mo surface. The high and sharp diffraction peak of (Fig. 4b) of the as-prepared $MoS_2$ samples indicates the formation of well-stacked layered structure of $MoS_2$ during the hydrothermal process. Our results agree well with findings of **(Wang et al., 2017).**
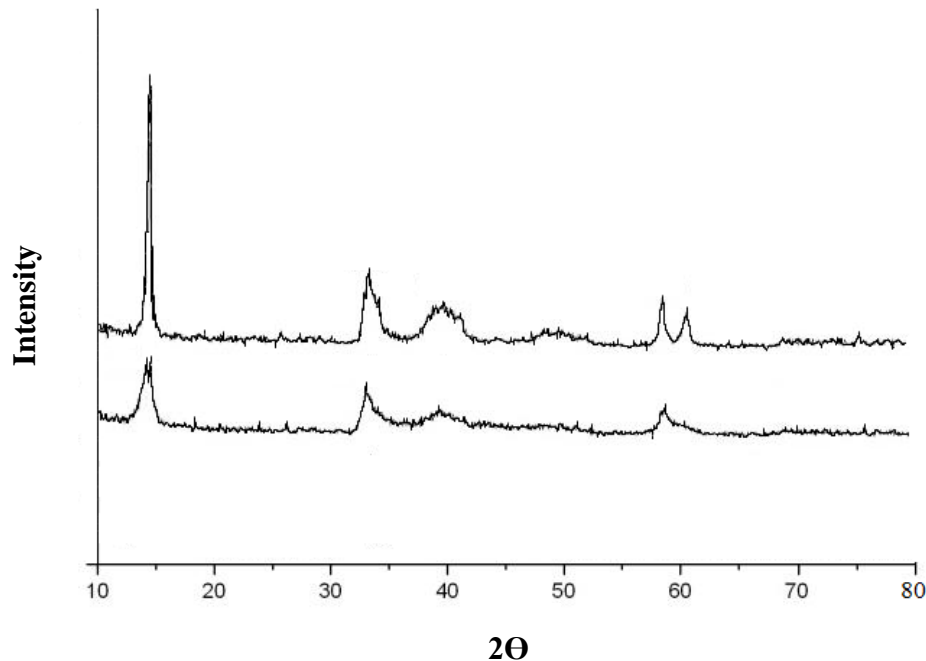
Figure (4): XRD images (a) at 280 ∘C & 25 bar and (b) at 280 ∘C & 35 bar.

### 3.1.3 EDX, SEM, and BET Measurements

EDX, SEM, and BET measurements were conducted after the best synthesized- temperature and pressure determined (as seen in Fig. 3b). Figure (5a) and (5b) shows images of EDX, and SEM for synthesized $MoS_2$. It is shown in Fig. (5a) that only the special feature of XRD peaks of hexagonal 2H-$MoS_2$ and no oxides Mo are revealed, which points out that the prepared MoS2 catalyst is indeed a complete sulfide catalyst. Image (5a) shows that the composition of $MoS_2$ catalyst is 14.39 wt% Mo and 85.61 wt % S indicating a typical composition of a pure $MoS_2$ catalyst. Figure (5b) for SEM images at 41.5 and 104 μm snapshots for the surface morphology of $MoS_2$ catalyst confirms the surface composed thoroughly of regular equal-sized particles. Table (2) list values of BET surface area and pore volume of MoS2 catalyst synthesized at different pressure and temperature. Table (2) depicted that the surface area and average pore size increase as the pressure and temperature are increase within the studied range in the present work. Catalyst surface area (Sg) is related to both pore volume (Vg) and average pore radius (a) by Eq.(3), cited in **Smith (1981).**

$$a = \frac{2V_g}{S_g} \qquad (3)$$

It is obvious from Eq. (2) that as Sg increased and a is decreased, Vg increases correspondingly to satisfy the relation of Eq.(2). **Wu et al. (2014)** studied the effect of synthesis temperature on characteristics of unsupported $MoS_2$ and $CoMoS_2$ catalysts for hydrodesulfurization of dibenzothiophene. The authors found that as synthesis temperature increased catalyst surface area increased while average pore diameter showed a different trend. **Wang et al. (2017)** synthesized $MoS_2$ nanocomposites by high pressure hydrothermal method. Wang et al. revealed that when the initial pressure increased from 2.5 to 3.5 Mpa, the corresponding surface area increased and all the morphologies of products are nanoflowers with a width of 10~20 nm. The published data have confirmed our experimental observations (see Table 2) for the effect of synthesis temperature and pressure on catalyst surface area and pore volume.
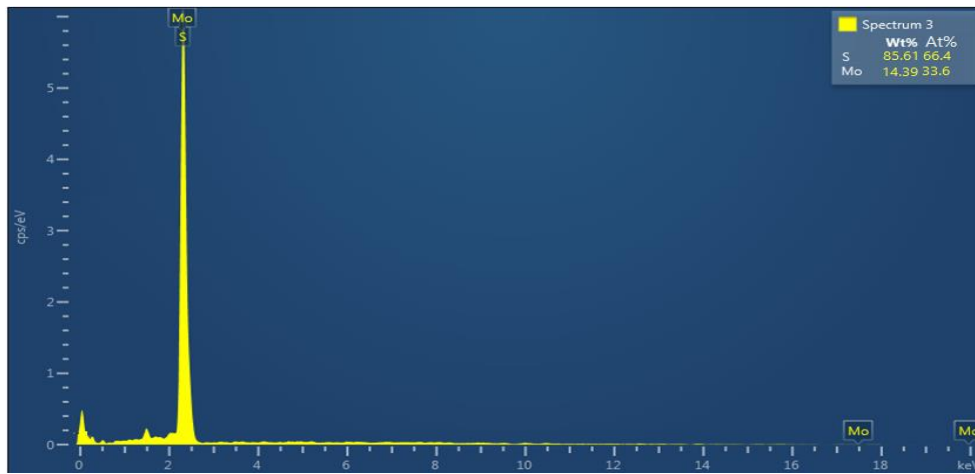
Figure (5a): EDX of MoS$_2$ catalyst synthesized at T= 320 oC, and P= 35 bar.

(i)
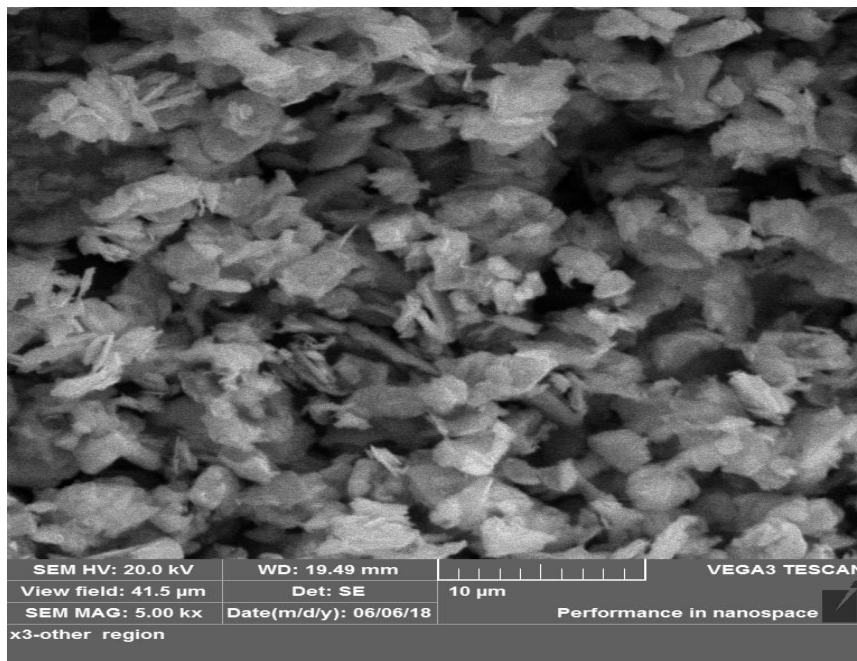
(ii)
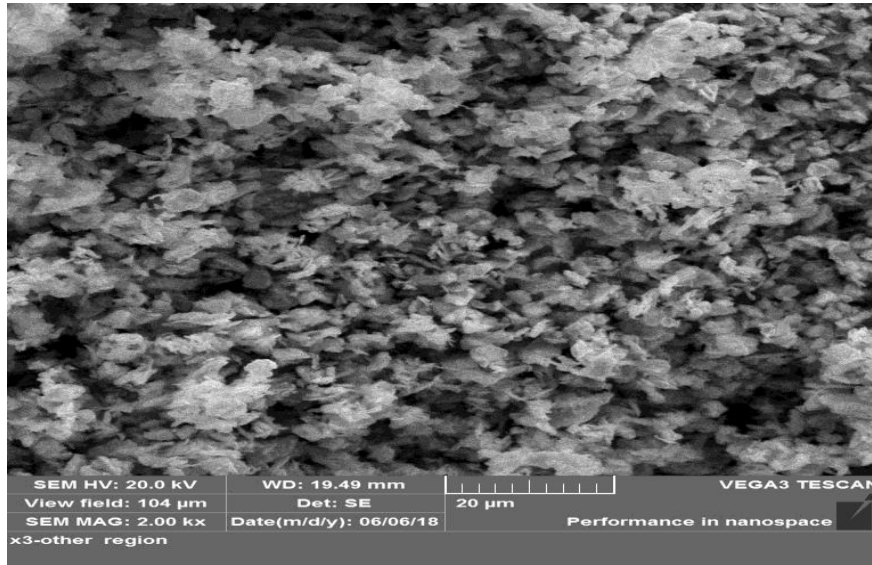


Figure (5b): SEM images (i) left, at 41.5 µm view; (ii) right, at 104 µm view

Table (2): BET measurements of $MoS_2$ catalyst synthesized at different synthesis conditions

| Property | 300 °C & 25 bar | 320 °C & 25 bar | 320 °C & 35 bar |
|---|---|---|---|
| Surface area, $m^2/g$ | 204.3 | 214.35 | 231.48 |
| Pore volume, $cm^3/g$ | 0.597 | 0.687 | 0.758 |

## 3. 2 KINETIC STUDY AND CATALYST ACTIVITY

The kinetic mechanism of HDS reaction on catalyst has a predominant effect on the activity of catalyst. **(Rabarihoela et al., 2009 and Chacón et al., 2012)** proposed a two site adsorption mechanism for S species and $H_2$ over the catalyst surface,

$$r_{HDS} = k \frac{K_S C_S}{1 + K_S C_S + K_{H2S} C_{H2S}} \times \frac{K_H C_H}{1 + K_H C_H} \tag{4}$$

Where, k is the reaction rate constant, $K_s$, $K_H$, and $K_{H2S}$ are the adsorption constant of $CH_4S$, $H_2$, and $H_2S$. $C_S$, $C_H$, and $C_{H2S}$ are the concentrations of sulfur compound, $H_2$, and $H_2S$. Since $H_2$ was in excess, $K_H C_H \gg 1$, and Eqn. (4) becomes

$$r_{HDS} = k \frac{K_S C_S}{1 + K_S C_S + K_{H2S} C_{H2S}} \tag{5}$$

If the sorption of $H_2S$ could be taken into account as greater than $C_4H_4S$ over the solid surface, then $(1 + K_{H2S} C_{H2S}) \gg K_S C_S$, Eqn. (5) becomes

$$r_{HDS} = k \frac{K_S C_S}{1 + K_{H2S} C_{H2S}} \tag{6}$$

The rate law of the HDS reaction is

$$r_{HDS} = k_{HDS} C_S \tag{7}$$

Where, $k_{HDS}$ is the specific rate constant containing the adsorption influence of $H_2S$. $C_s$ could be written as,

$$C_S = C_{SO}(1 - x_S) \tag{8}$$

Where, $C_{SO}$ and $x_S$ are the incipient weight content and conversion of sulfur, respectively

$$r_{HDS} = -\frac{dC_S}{dt} = \frac{dx_S}{dt} = k_{HDS}(1 - x_S) \tag{9}$$

Eqn. (9) is treated by integration and rearranged to obtain:

$$-ln(1 - x_s) = k_{HDS} t \tag{10}$$

$k_{HDS}$ is calculated by a graph of $-ln(1 - x_s)$ vs. t , where $k_{HDS}$ is represented by the slop. If the experimental result generated a straight line, this indicated a pseudo-first order trend. The required energy (Ea) to break down the R–S bond over the selected catalysts can be calculated from Arrehenius equation by plotting the left-hand side of Eqn. (11) against [1/T].

$$\ln k_{HDS} = (-Ea/R).(1/T) + \ln A \tag{11}$$

The applicability of pseudo first order kinetics was checked at three levels of temperature 300, 340, and 360 °C, while pressure was kept constant at 35 bar. As shown in Fig. (6), the plot of [–ln (1-xS)] versus [time] is linear, thus confirming that the pseudo first order kinetics could be used to represent the data. On the other hand, it can be clearly observed in Fig. (6) that an increase in the contact time caused a linear

increase in value of the term (–ln (1 – xS) value) whose slope represents the specific reaction rate over MoS2 catalyst at the studied reaction temperatures. It can also be seen in Figure (6) and Table 3, that the reaction rate constant raises as the catalyst activity increases. As a consequence, a higher conversion at various temperatures was found.
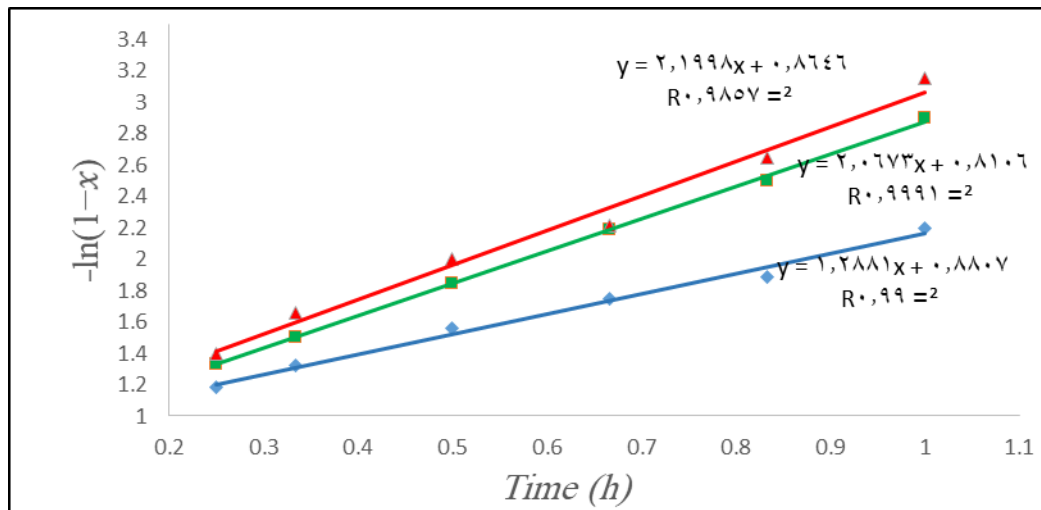


*Figure* (6): Plot of [–ln (1-x_S)] versus [time] at different temperatures.

Table (3): Values of k_HDS at different operating conditions

| Temperature (°C) | k_HDS (h$^{-1}$) |
|---|---|
| 300 | 1.288 |
| 340 | 2.067 |
| 360 | 2.199 |

The activation energies of HDS reactions over MoS$_2$ catalyst were calculated from the Arrhenius expression in Equ. (11). Slope of the line in Figure (7) represents the value of activation energy for HDS reaction over unsupported MoS$_2$ catalyst in terms of (– Ea/R). According to Figure (7), the activation energy (Ea) = 26.36 kJ/mol.



$$y = -3171.2x + 5.8014$$
$$R^2 = 0.9793$$
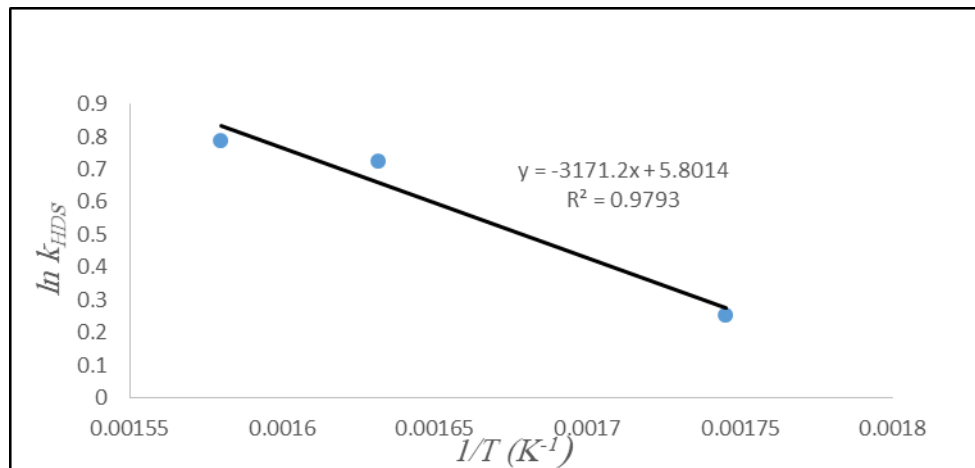
**Figure (7):** Plot between ($ln\ k_{HDS}$) versus ($1/T$).

Figure (8) illustrates the effects of temperature on sulfur removal from gas oil while other operating parameters were kept constant at (P=35 bar, WMoS2 = 0.5 gm). It can be observed that a positive relationship was established between sulfur removal and operating temperature. The sulfur removal, after 60 min of HDS reaction of gas oil, is 96.2, 95.8, and 88.0% at temperatures 360, 340, and 300 $^o$C respectively. This may be because of the equilibrium limitations at higher reaction temperatures for reversible HDS reactions. Moreover, Figure(8) illustrates a comparison between unsupported MoS$_2$ catalyst and supported CoMo/Al$_2$O$_3$ composed of 15.5 wt% Mo and 5.5 wt% Co, catalyst for HDS of Iraqi gas oil produced by Al-Daura Refinery, Baghdad **(Abid et al., 2018)**. As can be observed, MoS$_2$ catalyst offers 7.3% increasing in sulfur removal over CoMo/Al2O3 although the later catalyst has a higher weight percentage of Mo with 5.5 wt% of the promoter (i.e., Co).
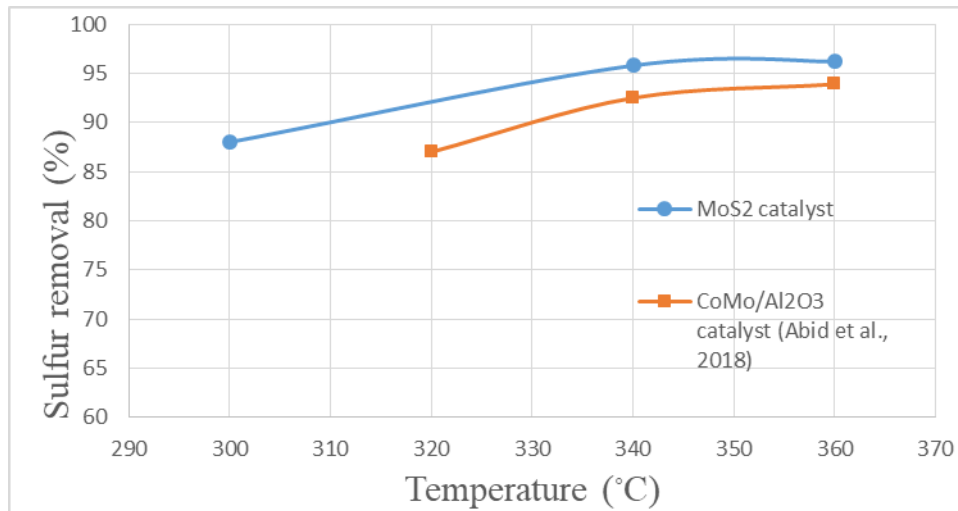
Figure (8): Variation of sulfur removal against temperature after 60 min of HDS reaction of gas oil for $MoS_2$ catalyst (present work) and $CoMo/Al_2O_3$ catalyst (Abid et al., 2018).

## 4. CONCLUSIONS

Unsupported $MoS_2$ catalysts were synthesized for the (HDS) of real feed gas oil using different temperatures and pressures in the hydrothermal method by utilizing molybdenum trioxide and sodium sulfide. The characterization of the catalyst was identified by XRD, SEM, and BET techniques. It was found that the BET surface and the pore volume were positively affected by pressure and temperature, which could improve the activity of MoS2. Kinetics analysis of the studied system depicted that the HDS reaction of gas oil over $MoS_2$ unsupported catalyst behaved as a pseudo-first order with the rate constant at 300,340, and 360 $^\circ$C equals to 1.288,1.96, and 2.14 hr-1, respectively and has activation energy = 26.36 kJ/mol. Experimental results revealed that the HDS activity of the unsupported $MoS_2$ catalyst was predominant over supported $CoMo/Al_2O_3$ catalyst under the same operating conditions.

## ACKNOWLEDGEMENT

## REFERENCES

**1.Abid M. F., Ahmed S. M.,Abdullah M.K.., Ali S. M.**, Experimental Study on Catalyst Deactivation by Nitrogen Compounds in a Hydroprocessing Reactor", *The Arabian Journal for Science and Engineering* (2018) 43:2133–2143

**2.Alvarez L., Berhault G., Alonso-Nunez G**. Unsupported NiMo sulfide catalysts obtained from nickel/ammonium and nickel/tetraalkylammonium thiomolybdates: Synthesis and application in the hydrodesulfurization of dibenzothiophene. Catalysis Letters. 2008 Sep 1; 125(1-2):35.

**3.Chang L., Yang H., Li J., Fu W., Du Y., Du K., Yu Q., Xu J., Li M**. Simple synthesis and characteristics of Mo/MoS2 inorganic fullerene-like and actinomorphic nanospheres with core–shell structure. Nanotechnology. 2006 Jul 6; 17(15):3827.

**4.Chacón R., Canale A., Bouza A., Sánchez Y.** Modeling of a three-phase reactorfor bitumen-derived gas oil hydrotreating. Brazilian Journal of Chemical Engineering. 2012; 9(1): 135-46.

**5.Choi J.M., Kim S.H., Lee S.J., Kim S.S**. Effects of Pressure and Temperature in Hydrothermal Preparation of MoS 2 Catalyst for Methanation Reaction. Catalysis Letters. 2018:1-2.

**6.Dhas N.A., Suslick K.S**. Sonochemical preparation of hollow nanospheres and hollow nanocrystals. Journal of the American Chemical Society. 2005 Mar 2; 127(8):2368-9.

**7.Duphil D., Bastide S., Lévy-Clément C**. Chemical synthesis of molybdenum disulfide nanoparticles in an organic solution. Journal of Materials Chemistry. 2002; 12(8):2430-2.

**8.Eijsbouts S., Mayo S.W., Fujita K**. Unsupported transition metal sulfide catalysts: From fundamentals to industrial application. Applied Catalysis A: General. 2007 Apr 16; 322:58-66.

**9.Gaojun A.N., Changbo L.U., Chunhua X.,** Production of Clean Diesel Fuel by the Efficient Hydrotreating Technology, The Second China Energy Scientist Forum, Beijing (2010).

**10.Girgis M.J., Gates B.C**. Reactivities, reaction networks, and kinetics in high-pressure catalytic hydroprocessing. Industrial & Engineering Chemistry Research. 1991 Sep; 30(9):2021-58.

**11.He Z., Que W**. Molybdenum disulfide nanomaterials: structures, properties, synthesis and recent progress on hydrogen evolution reaction. Applied Materials Today. 2016 Jun 1; 3:23-56.

**12.Hensen E.J., Kooyman P.V., Van der Meer Y., Van der Kraan A.M., De Beer V.H., Van Veen J.A., Van Santen R.A**. The relation between morphology and hydrotreating activity for supported MoS2 particles. Journal of Catalysis. 2001 Apr 25; 199(2):224-35.

**13.Rabarihoela V., Diehl F., Brunet S.** Deep HDS of Diesel Fuel: InhibitingEffect of Nitrogen Compounds on the Transformation of the Refractory 4,6-Dimethyldibenzothiophene Over a NiMoP/Al2O3 Catalyst, Catal Lett. 2009; 129: 50–60.

**14.Schweiger H., Raybaud P., Kresse G., Toulhoat H**. Shape and edge sites modifications of MoS2 catalytic nanoparticles induced by working conditions: a theoretical study. Journal of Catalysis. 2002 Apr 1; 207(1):76-87.

**15.Smith J.M.** Chemical Engineering Kinetics, third edition, McGraw-Hill International Editions, Singapore (1981).

16.**Speight J.G., Ozum B.**, editors. Petroleum refining processes. CRC Press; 2001 Oct 31.

17.**Théodet  M.,** 2010. New generation of" bulk" catalyst precursors for hydrodesulfurization synthesized in supercritical fluids (Doctoral dissertation, Université Sciences et Technologies-Bordeaux I).

18.**Wang Y., Lla X., Wang C**. Synthesis and Characterization of MoS2 Nanocomposites by a High Pressure Hydrothermal Method. Journal of Non-Oxide Glasses Vol. 2017 Apr 1; 9(2):47-54.

19.**Wu Z., Zhu W., Wang D., Whiffen V.M.L., Smith  K. J**. Effect of Annealing Temperature on Co–MoS2 Nanosheets for Hydrodesulfurization of Dibenzothiophene, Catal Lett (2014) 144:261–267.

20.**Zhang H., Lin H., Zheng Y., Hu Y., MacLennan A**. Understanding of the effect of synthesis temperature on the crystallization and activity of nano-MoS2 catalyst. Applied Catalysis B: Environmental. 2015 Apr 1; 165: 537-46.